Theoretical and Experimental Studies of Cycloconjugation Involving Second-Row Elements

Gideon Fraenkel,* Christopher J. Kolp, and Albert Chow

Contribution from the Department of Chemistry, The Ohio State University, Columbus, Ohio 43210. *Received December 7, 1990*

Abstract: In a method proposed to investigate conjugative interactions between second-row elements (S, P) amd a π-electron system, barriers to amide rotation have been measured using NMR line-shape methods, for *N*-acetyl-4-X(hetero)-1,4-dihydropyridines (X = SO_2, **7**; $P(O)OCH_3$, **13**; $C(CH_3)_2$, **6** (reference)) as well as the dihydro (**8a**) and tetrahydro (**9**) derivatives, respectively, of **7**. It is suggested that such interactions would stabilize the transition states for amide rotation by cycloconjugation but not the planar equilibrium states, compressing the barriers relative to reference **6**. In fact, amide barriers in **7**, **13**, and *N*-acetylpyrrole are substantially (>6 kcal) *less* than in **6**, **8ab**, and **9**, all ca. 17 kcal, in all of which saturated centers interrupt possible cycloconjugation. These conclusions are supported by the results of ab initio calculations at the Hartree–Fock level with the 3-21G(*) basis set.

The nature of the interactions between second-row elements, such as sulfur[1,2] or phosphorus,[1,3] with carbon π-electron systems has been the subject of extensive experimental and theoretical investigation.

A conjugative interaction of sulfone across the ends of a pentadienylic anionic loop was implicated from studies, undertaken by the Pagani group, of acidities of substituted 2*H*-thiopyran 1,1-dioxides,[4] (**1**) of chemical shifts in the corresponding anions[5] (**2**), as well as from crystallography of thiopyranylidine-dihydropyridine *S*,*S*-dioxide (**3**).[6b] The latter was concluded to

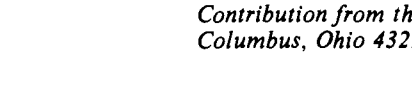

1 **2**

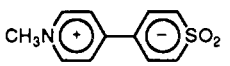

3

exist in the ylidic structure.[6a] The preceding evidence, together with work on related compounds,[7] reveals a pattern of cycloconjugation originally proposed by Moffit and Koch[8] for **4**.

4

In this paper we exploit the extreme sensitivity of the electronic energy of cyclic π-electron species to the number of π electrons associated with the ring in order to assess the possible operation of orbital overlap between selected second-row atoms (P, S) and the π system. Our procedure here is to compare barriers to amide rotation, determined by NMR line-shape analysis,[9] in 1-acetyl-4-hetero-1,4-dihydropyridines (**5**), where the heteroatom may be S or P, suitably substituted, with the corresponding barrier in reference compound 1-acetyl-4,4-dimethyl-1,4-dihydropyridine (**6a**). In the latter compound, the ends of the 3-aza-1,4-dienyl loop are joined by a saturated insulator. Consider the equilibrium (ground) and twisted transition states for amide rotation in these molecules, **5** and **6**. For brevity below we shall refer to the

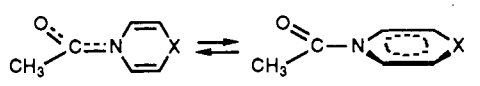

5a **5b**

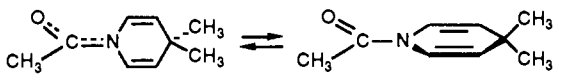

6a **6b**

optimized equilibrium state from a Hartree–Fock calculation as the ground state.

In the ground states we assume normal conjugation within the amide moiety leaves five electrons associated with the ring, whereas in the transition state for rotation the nonbonding electrons in nitrogen become part of a six π-electron system associated with the ring, **5b** and **6b**. To the extent that the heteroatom in the transition state, **5b**, overlaps with the π-loop, that species will be stabilized compared to the reference transition state, **6b**, in twisted amide where such overlap is not possible. In such a case the barrier to amide rotation in the hetero species, **5a** → **5b**, will be less than for the reference compound. To distinguish between possible transition-state cycloconjugation from long-range polarization effects due to the hetero entity, we can hydrogenate one of the double bonds in **5a**, then measure the barrier to amide rotation anew. Reduction preserves the inductive influence from the hetero entity but interrupts cycloconjugation.

Concomitant to these experimental measurements of amide barriers, we have undertaken some calculations, ab initio, of these processes to gain insight into the nature of the interactions between heteroatom and π system.

We have already reported preliminary results from an X-ray crystallographic and NMR study of 1-acetyl-4,4-dioxy-1,4-thiazine, **7**, which qualitatively confirms the above proposal.[16]

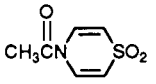

7

(1) Reviewed in: Kwart, H.; King, K. *d-Orbitals in the Chemistry of Silicon, Phosphorus and Sulfur*; Springer: Weinheim, 1977.
(2) Block, E. *Reactions of Organosulfur Compounds*; Academic Press: New York, 1978; pp 18–23.
(3) (a) Samitov, Yu Yu; Safiullin, R. K. *J. Gen. Chem. USSR* **1988**, *58*, 258. (b) *Zh. Obsch. Khim.* **1988**, *58*, 295. (c) Summarized in: Quin, L. D. *The Heterocyclic Chemistry of Phosphorus*; Wiley-Interscience: New York, 1981; pp 390–417.
(4) Pagani, G.; Garavaghi, G. *J. Chem. Soc., Perkin Trans. 2* **1973**, 50.
(5) Bradamente, S.; Mangia, S. A.; Pagani, G. *Tetetrahedron Lett.* **1970**, 3381.
(6) (a) Andreeti, G. D.; Bocelli, G.; Squarabotto, P. *J. Chem. Soc., Perkin Trans. 2* **1973**, 1189. (b) Pagani, G. *Ibid.* **1973**, 1184.
(7) (a) Bradamente, S.; Mairoana, S.; Mangia, A.; Pagani, G. *J. Chem. Soc. B* **1971**, 74. (b) Pagani, G.; Bradamente, S. *Tetrahedron Lett.* **1968**, 1041. (c) Pagani, G. *J. Chem. Soc. Perkin Trans. 2* **1974**, 1389.
(8) Moffit, W. E.; Koch, T. *Trans. Faraday Soc.* **1951**, *47*, 7.
(9) (a) Fraenkel, G.; Kaplan, J. I. *J. Am. Chem. Soc.* **1972**, *94*, 2907. (b) Kaplan, J. I.; Fraenkel, G. *NMR of Chemically Exchanging Systems*; Academic Press: New York, 1980; Chapter 6.
(10) Verboom, W.; Sukhai, R. S.; Meyer, J. *Synthesis* **1979**, 47; other examples of dihydro derivatives of **7**.
(11) Maillard, J.; Vincent, M.; Delaunay, P.; Rapin, M.; Vo-Van-Tri; Remond, G. *Chim. Ther.* **1969**, *4*, 80; *N*-methyl analogue of **9**.
(12) Hasserodt, U.; Hunger, K.; Korte, F. *Tetrahedron* **1964**, *20*, 1593.
(13) Felcht, U. German Patent DE2919754A1, Nov 27, 1980.
(14) Chattha, M. S.; Aguiar *J. Org. Chem.* **1971**, *36*, 2719.
(15) PANIC; Bruker Scientific: Billerica MA, 1974.
(16) Fraenkel, G.; Chow, A.; Gallucci, J.; Rizvi, S. Q. A.; Wong, S. C.; Finkelstein, H. *J. Am. Chem. Soc.* **1986**, *108*, 5339.

0002-7863/92/1514-4307$03.00/0

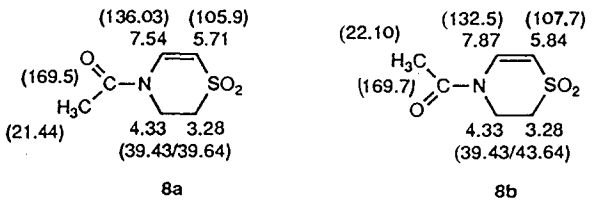

8a 8b

Figure 1. Proton and (^{13}C) NMR Chemical Shifts for **8a** and **8b** in acetone-d_6 at 261 K.

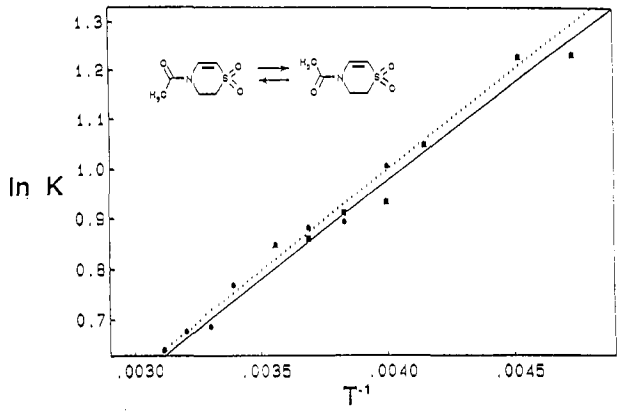

Figure 2. Hofmann plot, Equilibrium between rotational isomers **8a** and **8b**: NMR simulation (●, ...; integration (■,—).

In this paper we report NMR line-shape measurements of two hydrogenated derivatives of **7**, some work with a methoxyphosphorine oxide (**5a**, X = P(O)OCH$_3$) together with refined ab initio calculations of the amide barriers.

Results and Discussion

Partial hydrogenation[10] of **7** gave a mixture of the dihydro rotational isomers **8a** and **8b**. Their proton and ^{13}C chemical shifts

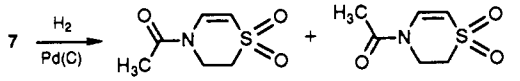

8a **8b**

at 241 K, summarized in Figure 1, are all different except for those due to methylenes. These two structures are assigned on the basis that proximity to oxygen deshields the resonance for the olefinic carbon ortho to nitrogen, **8a**, compared to proximity to methyl, **8b**. Then careful integration of the proton resonances under conditions of slow amide rotation, 211 K to 271 K, provides equilibrium constants for the **8a** ⇄ **8b** interconversion and the accompanying thermodynamic parameters (see Figure 2)

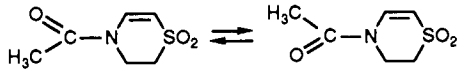

(1)

with $\Delta H = -0.8$ kcal and $\Delta S = -1.2$ eu, which are almost the same as values extracted from the proton NMR line-shape analysis, 261 K to 321 K, described below.

The olefinic protons in the two isomers **8a** and **8b** give rise to AX quartets which we label AX and A′X′. The deshielded doublets due to H ortho to nitrogen are slightly broadened by unresolved coupling to the CH_2 protons at C_6; see below. Above 250 K, with increasing temperature the resonances for the two rotamers progressively average due to faster rotation about the amide linkage. Line shapes for the deshielded olefinic proton resonances of **8a** and **8b** were calculated as a function of the rate of amide rotation.[9] Assuming that the proton spin states do not change during the rotation process, we treated the deshielded olefinic proton resonance as two identical independent unequally populated two-site exchanging systems. The centers of these two unequal doublets are separated by the vicinal coupling constant

(17) Dahlquist, K. I.; Forsen, S. *J. Phys. Chem.* **1969**, *73*, 4124.

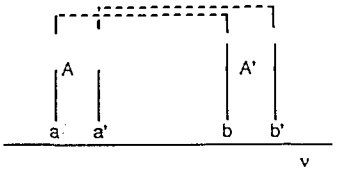

Figure 3. Deshielded olefinic proton resonances of **8a** and **8b**; dotted lines connect transitions which undergo signal averaging.

of 9.6 Hz; see Figure 3. Because of overlap of the resonances, it is convenient to combine the density matrix equations for both averaging doublets and then solve the resulting four equations for the four pseudo-half-spin transition elements $\rho_{a'}$, $\rho_{b'}$, ρ_a, and ρ_b, as a function of frequency, where a and b refer to one doublet, a′ and b′ to the other. Then the absorption is obtained from the summation:

$$\text{abs}(\Delta\nu) = -\text{Im}((A)\rho_a + (A)\rho_{a'} + (B)\rho_b + (B)\rho_{b'}) \quad (2)$$

each transition element weighted by its corresponding rotamer concentration, (A) or (B), for **8a** or **8b**, respectively.

The four coupled first-order density matrix equations in the ρ elements take the form

$$(i2\Pi\Delta\nu + A)\rho_{\text{col}} = iCB_{\text{col}} \quad (3)$$

where $\Delta\nu$ is the frequency point, ρ_{col} the half-spin elements, C a constant, B the column 1, 1, 1, 1, and A the coefficient matrix given in (4). The latter contains the four internal shifts $\Delta\nu_a$ to $\Delta\nu_{b'}$, line-width parameter $1/T$, and forward and reverse rate constants k_f and k_r (s^{-1}), respectively. Since both the equilibrium

$$\begin{bmatrix} i2\Pi\Delta\nu_a - \frac{1}{T} & k_f & 0 & 0 \\ -k_f & i2\Pi\Delta\nu_b - \frac{1}{T} & 0 & 0 \\ k_r & -k_r & i2\Pi\Delta\nu_{a'} - \frac{1}{T} & 0 \\ 0 & 0 & -k_f & i2\Pi\Delta\nu_{b'} - k_r - \frac{1}{T} \\ 0 & 0 & k_r & -k_r \end{bmatrix} \quad (4)$$

constant k_f/k_r and the separation between the a,a′ and b,b′ doublets vary with temperature, it was necessary to estimate their values by extrapolation from the temperature range within which NMR is independent of the rate of amide rotation into the range where signal averaging becomes significant. The observed olefinic ortho to N proton resonances are displayed together with the line shapes calculated to fit them in Figure 4. Figure 5 shows the Eyring plots for the forward and reverse rotations, the results being summarized in Figure 6.

An altenative procedure to investigate possible cycloconjugation in acetyl dioxy thiazine **7** is to fully hydrogenate this compound, then measure the barrier to acetyl rotation in the resulting 1-acetyl-4,4-dioxy-4-thiamorpholine. Reduction of **7** was accomplished using H_2 and 5% Pd on C. Carbon-13 NMR of the resulting **9** at 303 K shows all carbons to be magnetically non-

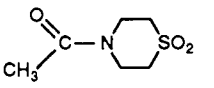

9

equivalent; see Figure 7. Clearly, at this temperature, rotation about the amide linkage is slow relative to the NMR time scale; for example, the shift between the carbons ortho to nitrogen is 303.2 Hz at 62.9 MHz. With increasing temperature, these resonances from the two sides of the ring progressively undergo signal averaging o with o' and m with m'; see Figure 8.

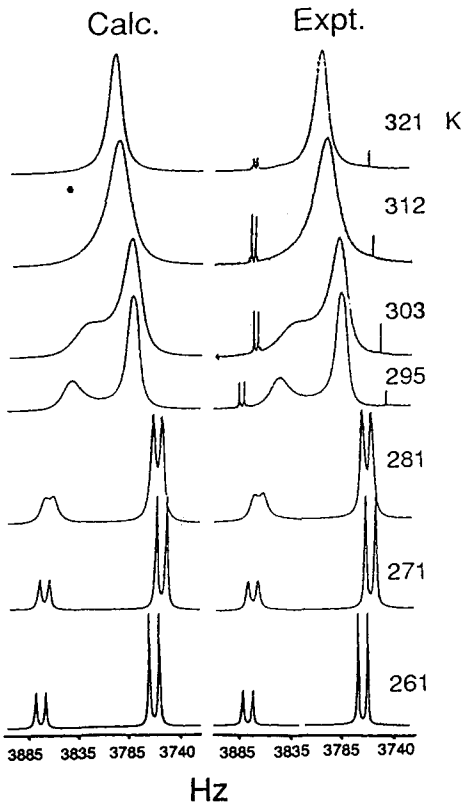

Figure 4. Proton NMR, 500 MHz, **8a** ⇄ **8b**, mixture, 0.21 M in acetone-d_6, HCN vinyl resonance: (right) experimental, different temperatures; (left) calculated.

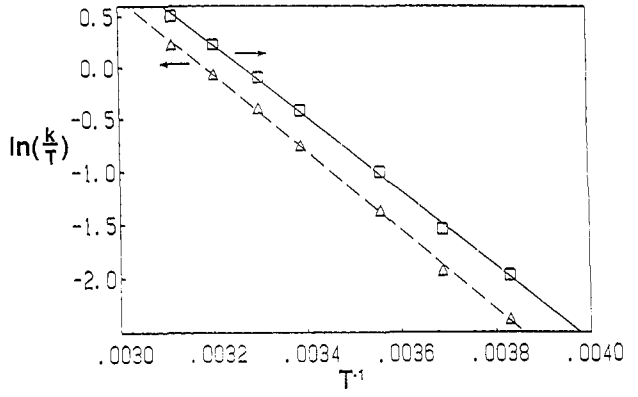

Figure 5. Eyring plot for the interconversion **8a** ⇄ **8b**, 0.21 M in acetone-d_6: (■) forward, (△) reverse.

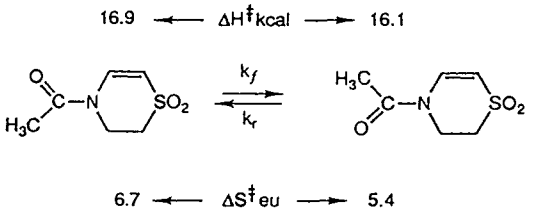

Figure 6. Activation parameters for the **8a** ⇄ **8b** interconversion.

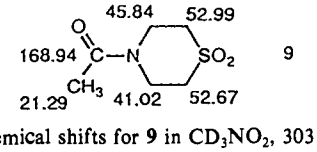

Figure 7. ^{13}C chemical shifts for **9** in CD_3NO_2, 303 K.

The rate of amide rotation in **9** was obtained via line-shape analysis of the meta to nitrogen ring ^{13}C resonances. This averaging doublet, m with m', was treated as an equally populated half-spin exchanging system. Although the intrinsic shifts vary with temperature, the difference $\delta_m - \delta_{m'}$ changes relatively little. Figure 8 shows experimental spectra with line shapes calculated to reproduce them. This procedure gave a $\Delta H^{\ddagger}$ of 17.8 kcal with

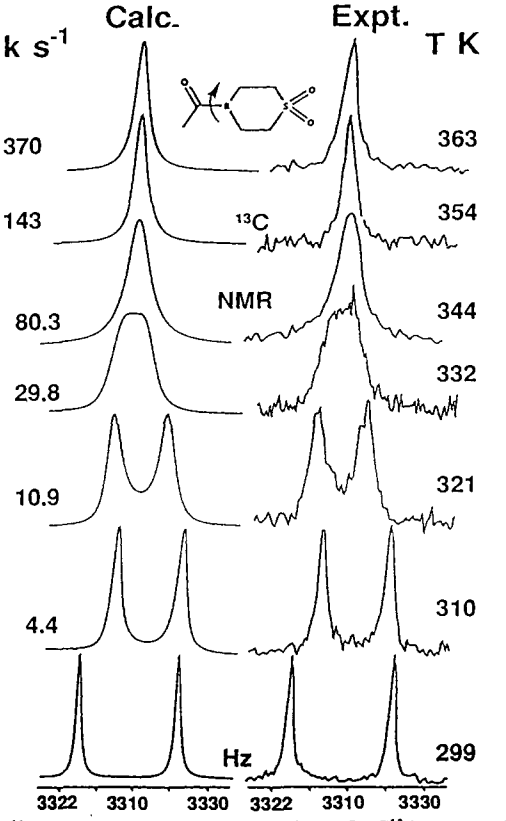

Figure 8. ^{13}C NMR, 62.9 MHz, **9**, 1.1 M CD_3NO_2, $S^{13}CH_2$ part: (right) observed, different temperatures; (left) calculated line shapes with fitted rate constants.

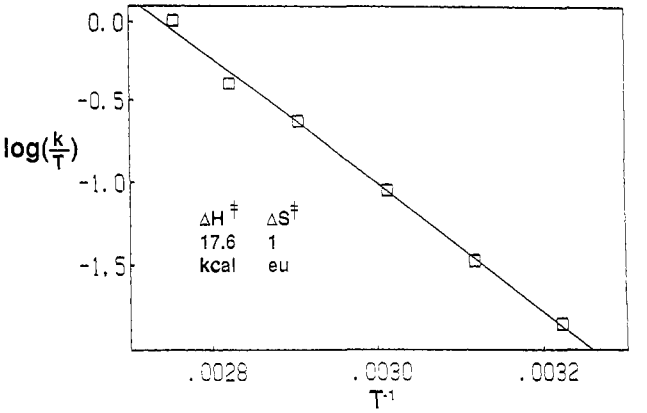

Figure 9. Eyring plot for acetyl rotation in **9**, 1.1 M in CD_3NO_2.

Scheme I[a]

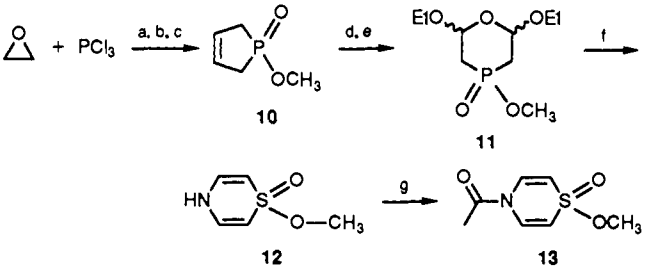

[a] (a) Copper stearate, 0 °C; (b) 1,3-Butadiene, 100°, 12 h, bomb; (c) CH_3OH, −10°; (d) O_3, EtOH–CH_2Cl_2, −78°; (e) SO_2; (f) NH_4Cl; (g) Ac_2O, reflux.

Table I. NMR, ^1H, and (^{13}C) of 4-Hetero-1,4-dihydropyridines (shifts, δ units; J, Hz; C_2 syn to O in amides)

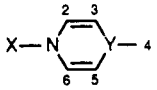

	184 K	300 K	300 K	300 K	300 K	182 K	273 K
solv	$(CD_3)_2CO$	$(CD_3)_2SO$	(CH_3OD)	$(CD_3)_2SO$	(DMSO THF)	$(CD_3)_2CO$	$(CD_3)_2CO$
Y	$P(O)OCH_3$	$P(O)OCH_3$	$P(O)OCH_3$	SO_2	SO_2	SO_2	$C(CH_3)_2$
NX	$NC(O)CH_3$	$N:^-K^+$	NH	NH	$N:^-K^+$	$NC(O)CH_3$	$NC(O)CH_3$
	13	*a*	**12**	*b*	*c*	**7**	**6**
δ_x	2.62		8.23	9.08		2.05	2.1
	(170.2)[d]					(166.79)[d]	(169.0)[d]
	(22.3)[e]					(21.70)[e]	(22.0)[e]
δ_2	8.221	7.38	7.17	7.011	8.79	8.04	7.02
	(141.6)	(153.47)	(141.9)	(133.49)	(145.77)	(131.2)	(137.0)
δ_3	5.625	4.40	5.10	5.94	5.48	6.51	4.79
	(99.7)	(86.9)	(91.84)	(104.94)	(99.56)	(109.8)	(103.0)
δ_5	5.474	4.40	5.10	5.94	5.48	6.41	4.89
	(97.62)	(86.9)	(98.84)	(104.94)	(99.56)	(102.52)	(103.0)
δ_6	8.099	7.38	7.17	7.01	8.79	7.92	6.65
	(137.4)	(153.49)	(141.9)	(133.49)	(145.77)	(127.72)	(137.0)
J							
2,3	11.4	9.51	10.6	8.92	7.7	9.66	8.45
2,4[f]	31.2	33.1	28.8				
	(<0.5)	(<0.5)	(<0.5)				
2,5	−0.02	−0.2	g	0.04		−0.24	−0.20
2,6	2.55	1.52	g	1.9	0.76	4.76	1.74
3,4[c]	1.61	1.8	g				
	(129.5)	(129.1)	(131.4)				
3,5	4.08	4.43	g	4.45	4.51	2.61	2.72
3,6	−0.02	−0.02	g	0.04		−0.11	0.11
4,5[c]	1.1	1.8					
	(129.6)	(129.1)	(131.4)				
4,6	29.1	31.1	28.8				
	(<0.5)	(<0.5)	(<0.5)				
5,6	11.21	9.51	10.6	8.92	7.70	9.66	8.45

[a] Potassium salt of **12**. [b] 4*H*-1,4-Thiazine 1,1-dioxide.[16] [c] Potassium salt, 4*H*-1,4-thiazine 1,1-dioxide. [d] Carbonyl ^{13}C shift. [e] Methyl. [f] Coupling to ^{31}P. [g] Not resolved.

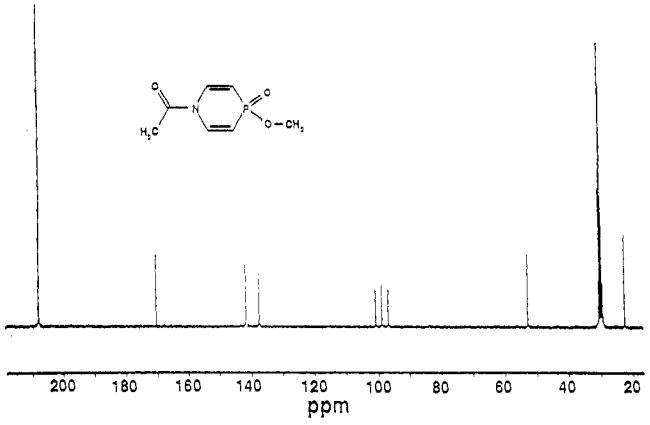

Figure 10. ^{13}C NMR for **13** in acetone-d_6, 196 K.

$\Delta S^\ddagger = +1.1$ eu as determined from the Eyring plot in Figure 9.

In chemistry to obtain a phosphorus derivative of **5**, a modification of Felcht's procedure[12,13] furnished the known 1-methoxy-3-phosphene 1-oxide (**10**); see Scheme I. Ozonolysis of **10** using standard conditions (−78 °C, ethanol, CH_2Cl_2, then SO_2),[14] followed by condensation of the resulting crude cyclic bis-acetal (**11**), with ammonium chloride in acetic acid, produced 4-methoxy-1,4-azaphosphorine 4-oxide (**12**), identified via its NMR spectra (see Table I) and MS behavior. Finally, acylation of **12** in acetic anhydride produced the required 1-acetyl-4-methoxy-1,4-azaphosphorine 4-oxide (**13**) (see Table I and Scheme I). NMR, both proton and ^{13}C of **13** in acetone-d_6 at 184 K, shows all ring carbons and protons to be magnetically nonequivalent. Proton NMR was analyzed using PANIC;[15] the results are listed in Table I and spectra shown in Figures 10 and 11. Above 184 K, with increasing temperature, the resonances for H_2 and H_6 signal average as do, separately, those for H_3 and H_5 due to progressively faster rotation about the amide linkage; see Figure 12a,b. Comparison of experimental spectra with line shapes calculated as a function of the rate of amide rotation provided the rates of rotation (Figure 12a). This procedure was carried out separately for the resonance of olefinic protons in **13** ortho to nitrogen and those meta to nitrogen. The two treatments gave only slightly different activation parameters, still within experimental error and both with excellent correlation coefficients (Table II). Hence, the averaged activation parameters will be used: $\Delta H^\ddagger = 8.3$ kcal and $\Delta S^\ddagger = -12$ eu. Acetyl rotation in **13** with respect to the heterocycle plane can proceed via two transition states, one with the P=O and C=O oxygens cis and the other trans. The results reported here do not distinguish different rates of rotation via different paths. It may be that acetyl is too far from the

Table II. Activation Parameters for Acetyl Rotation in **13** in Acetone-d_6 from Olefinic Resonance

proton NMR resonance	$\Delta H^\ddagger$ kcal/mol	$\Delta S^\ddagger$, eu	lcc
H ortho to N	8.0	−14	0.9992
H meta to N	8.6	−10	0.9998

Table III. Experimental Barriers to Amide Rotation and Carbonyl Stretching Frequencies for All Relevant Compounds

	9	**14**	**13**	**7**	**8a**	**6**
$\Delta G^\ddagger$[a] (kcal/mol)	17	12.2	11.9	12	14.7	16.9
$\Delta H^\ddagger$ (kcal/mol)	17.3	12	8.3	11.7	16.5	17.2
$\Delta S^\ddagger$ (eu)	1	−0.6	−12	1	6	1
IR (cm^{-1})	1637	1735	1720.3	1735	1688	1700

[a] 298 K.

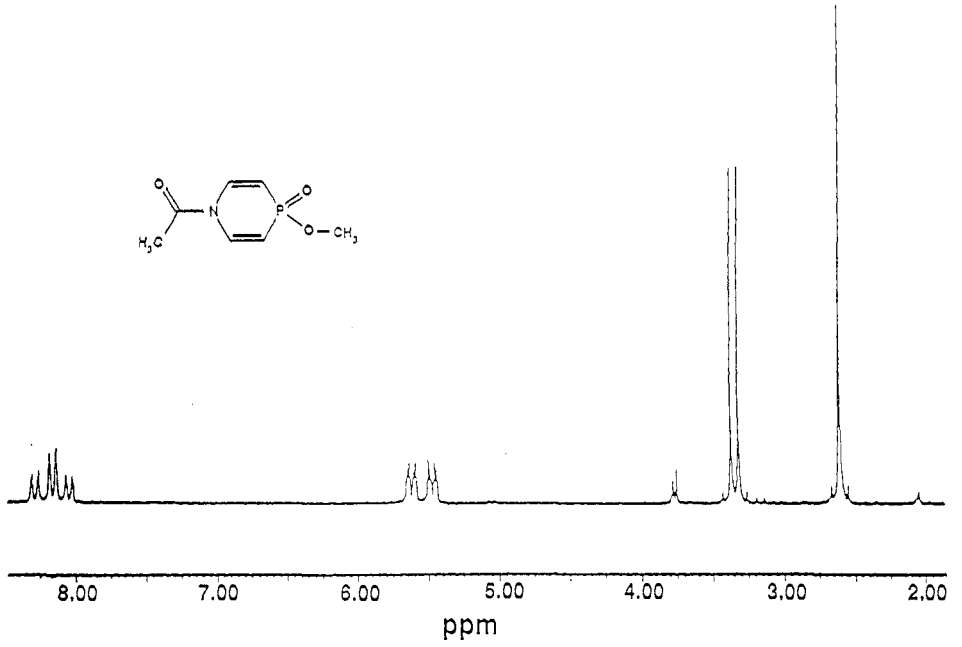

Figure 11. Proton NMR for **13** in acetone-d_6, 184 K.

Table IV. Calculated Barriers to Amide Rotation[a]

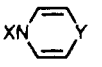

X	Y	barrier, kcal/mol	basis	g[b]	t[c]	compd
CHO	SO_2	11.31	STO-3G*	−858.321 43	−858.321 43	**15**
CHO	SO_2	17.85	3-21G(*)	−864.244 48	−864.215 82	**15**
CHO	SO_2	16.81	6-21G*	−868.328 78	−868.290 91	**15**
CHO	SO_2	18.03	6-31G*	−868.686 32	−868.657 60	**15**
CH_3CO	SO_2	12.13	3-21G(*)	−907.072 97	−907.050 25	**7**
CHO	CH_2	21.87	3-21G(*)	−358.560 42	−358.525 57	*d*
CH_3CO	CH_2	16.42	3-21G(*)	−397.360 58	−397.334 41	*e*
CH_3CO	$C(CH_3)_2$	16.92	3-21G(*)	−475.031 88	−475.002 99	**6**

[a] Geometry optimized. [b] Equilibrium energies (atomic units). [c] Twisted-state energies, amide plane 90° with respect to six-membered ring. [d] *N*-Formyl-1,4-dihydropyridine. [e] *N*-Acetyl-1,4-dihydropyridine.

substitution on phosphorus for these moieties to perturb each other, in which case the rotation rates would be the same.

Comparison of the amide barrier for *N*-acetyl-4,4-dioxy-1,4-thiazine (**7**), reported by us previously,[16] with those of its dihydro (**8a** and **8b**) and tetrahydro (**9**) derivatives, respectively, and dihydropyridine (**6**, Table III) reveals that all these barriers are very similar, ca. 17 ± 0.5 kcal/mol, except for **7**. All four compounds in which potential cycloconjugation interactions are interrupted by one or more saturated centers exhibit a common barrier of 17 kcal, seemingly independent of the 4-heteroatom. Apparently, long-range inductive interactions cannot be responsible for the much lower barrier of ca. 12 kcal/mol in **7**. Then, using the barrier of 17 kcal/mol as a reference for minimal transition-state cycloconjugation, thiazine (**7**), *N*-acetylpyrrole (**14**), and 1-acetyl-4-methoxy-4-oxyphosphorine (**13**) are concluded to exhibit some degree of cycloconjugation in their transition states for amide rotation.

A theoretical investigation of these barriers was begun by approximating *N*-acetyl-dioxythiazine (**7**) as the *N*-formyl derivative **15**, and then calculating the barrier to amide rotation ab initio at several levels of refinement.

We previously reported the calculated amide barrier of **15** at

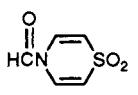

15

the STO-3G* level using GAUSSIAN 90[18] to be 12 kcal/mol,[16] within experimental error of that observed for **7**. Calculations for **15** were then carried out using the GAMESS[19] program. Input structure parameters came from a combination of literature values for other compounds and the results of X-ray crystallography of **7**.[16] The final equilibrium-state calculation was carried out with full geometry optimization. This calculation was repeated for the transition-state model in which the formyl group is constrained perpendicular to the azadienyl plane and the remaining structural parameters reoptimized with C_s symmetry.

(18) (a) Hehre, W. J.; Stewart, R. F.; Pople, J. A. *J. Chem. Phys.* **1969**, *51*, 2657. (b) Hehre, W. J.; Ditchfield, R.; Stewart, R. F.; Pople, J. A. *J. Chem. Phys.* **1970**, *52*, 2769. (c) Ditchfield, R.; Hehre, W. J.; Pople, J. A. *J. Chem. Phys.* **1970**, *52*, 5001. (d) Ditchfield, R.; Hehre, W. J.; Pople, J. A. *J. Chem. Phys.* **1971**, *54*, 724. (e) Binkley, J. S.; Pople, J. A.; Hehre, W. J. *J. Am. Chem. Soc.* **1980**, *102*, 939.

(19) (a) Dupuis, M.; Spangler, D.; Wendoloski, J. J. *National Resource for Computations in Chemistry Catalog*; University of California: Berkeley, CA, 1980; Program QG01. (b) Schmidt, M. W.; Boatz, J. A.; Baldridge, K. K.; Koseki, S.; Gordon, M. S.; Elbert, S. T.; Lam, B. *QCPE Bull.* **1987**, *7*, 115.

(20) Magnusson, E. *J. Am. Chem. Soc.* **1990**, *112*, 7940–7951.

(21) Reed, A. E.; Schleyer, P. v. R. *J. Am. Chem. Soc.* **1990**, *112*, 1434–1445.

(22) Shambayati, S.; Blake, J. F.; Wierschke, S. G.; Jorgensen, W. L.; Schreiber, S. L. *J. Am. Chem. Soc.* **1990**, *112*, 697–703.

(23) Wiberg, K. B.; Laidig, K. E. *J. Am. Chem. Soc.* **1987**, *109*, 5935.

(24) Boche, G.; Eiben, R.; Thiel, W. *Angew. Chem., Int. Ed. Engl.* **1982**, *21*, 688. Boche, G.; Bosold, F.; Eiben, R. *Ibid.* **1984**, *23*, 797.

(25) Arthurs, M.; Al-Daffaee, H. K.; Haslop, J.; Kubal, G.; Pearson, M. M.; Thatcher, P. *J. Chem. Soc., Dalton Trans.* **1987**, 2615.

(26) Supowit, A.; Johnson, W.; Chow, A. SPECTRAL ANALYSIS; Instruction and Research Computer Center: The Ohio State University, 1974.

(27) Noland, W. E.; Demaster, R. D. *Org. Syn.* **1972**, *52*, 135.

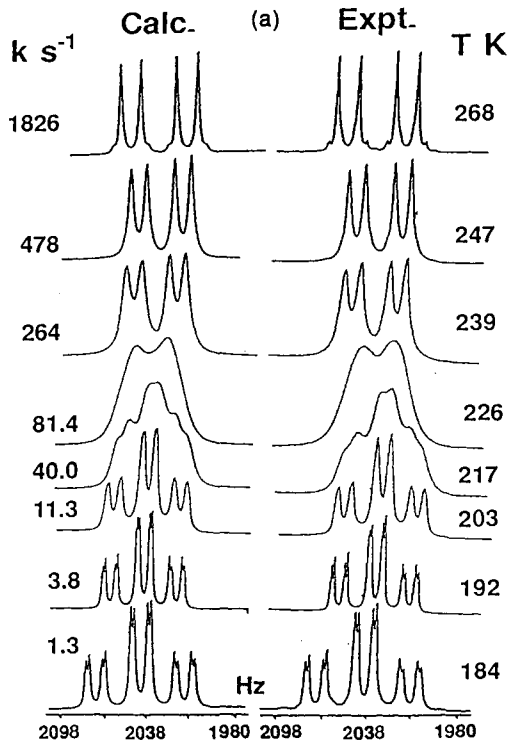

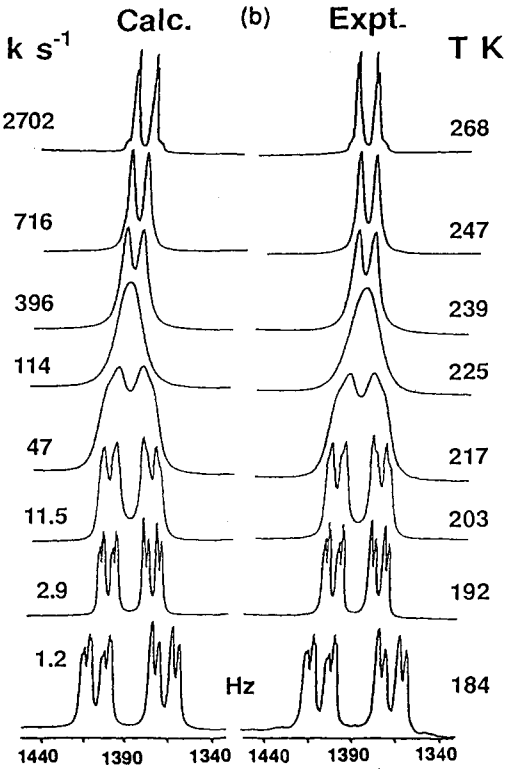

Figure 12. Proton NMR (250 MHz) for **13** in acetone-d_6. (a) Deshielded olefinic resonance: (left) calculated with fitted rate constants; (right) experimental, with temperature (K). (b) Shielded olefinic resonance: (left) calculated with fitted rate constants; (right) experimental, with temperature (K).

As seen in Table IV, as the level of refinement improves from STO-3G* to 6-31G*, the calculated barrier to amide rotation, fully geometry optimized, in **15** jumps from 11.7 kcal/mol to 17 kcal/mol. Thus, we learn that *N*-formyldioxythiazine (**15**) is an unsuitable model for **7**, further, that the barrier ceases to change significantly beyond the 3-21G(*) basis set. This then appears to be a reliable and economic level at which to carry out further

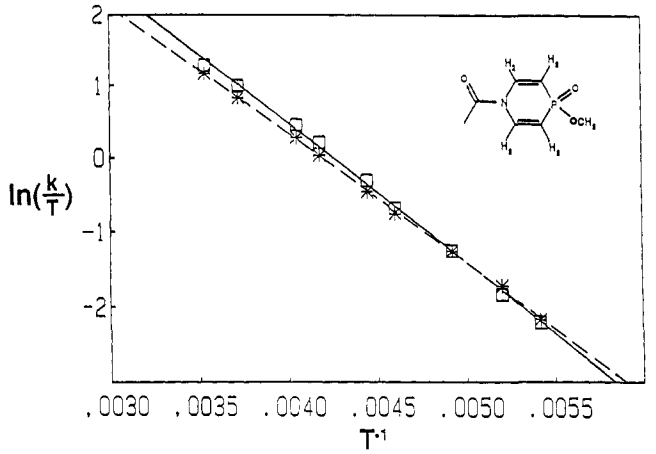

Figure 13. Eyring plot for amide rotation in **13** in acetone-d_6: asterisks and dashed line from H_2, H_6 resonance, deshielded; squares and solid line from H_3, H_5 resonance, shielded.

Table V. Compound **7**: Calculated, 3-21G(*), Bond Distances and Angles for Equilibrium (g) and Twisted State (t)

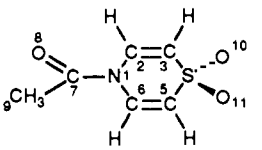

	bond distances, Å			bond angles	
	g	t		g	t
N–C_7	1.4109	1.4541	N_1–C_2–C_3	122.84	122.79
C_7–O_8	1.2077	1.1963	C_2–C_3–S_4	124.19	123.70
C_7–C_9	1.5110	1.5026	O_{10}–S_4–O_{11}	109.30	109.18
N–C_2	1.3930	1.3820	C_3–S_4–C_5	108.95	109.11
N–C_6	1.3916		S_4–C_5–C_6	124.20	123.70
C_2–C_3	1.3233	1.3253	C_5–C_6–N_1	122.97	122.79
C_5–C_6	1.3203		C_6–N_1–C_2	116.85	117.70
C_3–S	1.7265	1.7216	N_1–C_7–O_8	120.90	122.45
C_5–S	1.7168		N_1–C_7–C_9	117.34	113.18
S–O_5	1.4379	1.4392	O_8–C_7–C_9	121.76	124.37
S–O_6		1.4383			

Table VI. Compound **7**: Mulliken Overlap Population,[a-c] Equilibrium (g), and Twisted State (t) to Amide Rotation

		g[b]	t[b]
$C_3(2p_z)$	$S(3p_z)$	0.018835	0.0198
$C_5(2p_z)$	$S(3p_z)$		
$C_3(2p_z)$	$S(3d_{xz})$	0.004655	0.0047
$C_5(2p_z)$	$S(3d_{xz})$		
$N(2p_z)$	$C_2(2p_z)$	0.02366	0.0358
$N(2p_z)$	$C_6(2p_z)$		
$C_2(2p_z)$	$C_3(2p_z)$	0.23558	0.22621
$C_5(2p_z)$	$C_6(2p_z)$		

[a] Summed for all pairs of inner and outer functions. [b] Averaged over two sides of ring. [c] 3-21G(*).

calculations. Accordingly, the barrier to acetyl rotation in *N*-acetyldioxythiazine (**7**) was calculated at the Hartree–Fock level with 3-21G(*) basis (GAUSSIAN 90) in similar fashion to **15**, described above, starting with the crystallographic parameters as input for full optimization at the Hartree–Fock level. Then a frequency calculation was carried out at the 3-21G(*) level for the optimal geometry of **7**. All frequencies were found to be real, within 12% of the experimental ones,[28] indicating this configuration is an equilibrium state. This procedure gave rise to a calculated barrier of 12.13 kcal/mol within experimental error of the observed

(28) Hehre, W. J.; Schleyer, P. v. R.; Pople, J. A. *Ab Initio Molecular Orbital Theory*; Wiley Interscience: New York, 1986; p 236.

Table VII. Atomic Charges for Compound **7**, 3-21G(*)[a]

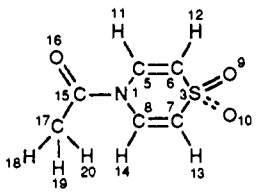

no.[b]	z, (g)	z, (t)	no.[b]	z, (g)	z, (t)
1 N	−1.0732	−1.0201	12 H	0.2968	0.2945
3 S	1.6515	1.6501	13 H	0.2990	0.2945
5 C	0.2041	0.2177	14 H	0.3352	0.2916
6 C	−0.7007	−0.7176	15 C	0.8733	0.7390
7 C	−0.7201	−0.7176	16 O	−0.5797	−0.4769
8 C	0.1981	0.2177	17 C	−0.7219	−0.6666
9 O	−0.5810	−0.5876	18 H	0.2866	0.2618
10 O	−0.5810	−0.5822	19 H	0.2539	0.2551
11 H	0.3053	0.2916	20 H	0.2539	0.2551

[a] Ground, g; twisted, t. [b] As in *Z* matrix.

value of 12 kcal/mol. The resulting structure parameters are listed in Table V and in the supplementary material. Mulliken populations for π overlap between selected pairs of functions are listed in Table VI. These values are small except for the C, C bond in the ring. Note that in the equilibrium state, the N-$(2p_z)$–$C_{2(5)}(2p_z)$ overlap is remarkably similar to that for S-$(3p_z)$–$C_{3(5)}(2p_z)$ interactions. Proceeding from equilibrium to twisted states, respectively, both values increase, the former by 48% and the latter by 5%. Also, whereas sulfur d functions have significant coefficients (0.1 to 0.2) in some higher occupied orbitals and contribute to the charge distribution, d–π overlap contributes only slightly to bonding (see Table VI), in contrast to the results from more approximate calculations.[16] This subject has been discussed in great detail in three recent papers.[20-22]

The calculated electron density distribution for **7** shows this to be a highly polar molecule (Table VII and supplementary material). Electron populations for the amide moiety are similar to Wiberg and Laidig's calculated values for formamide.[23] Using the calculated charges for the two states (g and t) for **6** and **7**, we find the difference beween the classical electrostatic contributions to the two barriers (for **6** minus that for **7**) to be 15 kcal/mol. This is the correct order and direction as that observed. It is also interesting that the corresponding potential energy difference from the ab initio calculations also comes out to be 15 kcal/mol. In sum, those results demonstrate the importance of electrostatic interactions within our compounds.

Interestingly, the calculated barrier for the model compound *N*-acetyl-4,4-dimethyl-1,4-dihydropyridine (**6**) (3-21G(*)) at 16.92 kcal/mol is similarly satisfactorily close to the observed value, 17.2 kcal/mol, and confirms the suitability of 3-21G(*) for our calculations which reproduce the experimental behavior. Further, note that the experimental barriers to amide rotation for the half- and fully hydrogenated derivatives of **8a**, **8b**, and **9** also are around 17 kcal/mol.

Experiments conceived along similar lines to those described above have been reported by Boche[24] et al., who used NMR to measure dynamics of rotation about the ring-carbonyl carbon bond in *N*,*N*-dimethyl carbonyl substituted carbanions: Cp^{1-}, cycloheptatrienyl^{1-}, and cyclononatetraenyl^{1-}. They found the Cp^{1-} species to rotate too fast to measure at −106 °C. Also the last, C_9^{1-} was concluded to exist with the substituent orthogonal to the ring. In contrast the C_7^{1-} species exhibited a larger barrier $\Delta G^{\ddagger}$ (70 °C) of 17.5 kcal/mol. Despite the use of approximate coalescence measurements[24,25] on ion-paired salts, these results clearly confirm the aromaticity of cyclic $4n + 2$ cyclic π-electron anions.

Conclusions

Barriers to amide rotation in 4-hetero-*N*-acetyl-1,4-dihydropyridines provide qualitative information on cycloconjugation of second-row heteroatoms (S and P) with the π-electron system. The maximum stabilization of the transition state to amide rotation in **7** (X = SO_2), ca. 6 kcal/mol, also is confirmed by ab initio calculations at the Hartree–Fock level of the barriers. Experiments with dihydro (**8**) and tetrahydro (**9**) derivatives of **7** show that long-range inductive interactions are not responsible for the low amide barrier in **7**.

Experimental Section

NMR Equipment. All NMR data were obtained using Bruker equipment-AM 250, MH 300 and MSL 300 spectrometers, with ^1H, ^{13}C, and ^{31}P at 250 or 300, 62.9 or 75.5, and 101 MHz, respectively.

NMR Line-Shape Analysis.[9] As noted above, the resonance for olefinic hydrogens ortho to nitrogen in **8a** and **8b** is treated as two identical unequally populated two-site exchanging systems whose centers are separated by the proton vicinal coupling of 9.6 Hz. Since the shifts vary linearly with temperature according to

$$\Delta\nu_{a,a'} = -4.33T + 17070 \quad (5)$$

$$\Delta\nu_{b,b'} = -2.27T + 8830 \quad (6)$$

it was necessary to estimate their values by extrapolating from the temperature range, 210 K to 270 K, wherein the center of gravity of the doublets was unaffected by amide rotation to the range where signal averaging takes place. In like fashion, equilibrium constants for the signal averaging temperature range were extrapolated from the right side of the Hofmann plot. Given the intrinsic NMR parameters and K_{eq} (k_f/k_r), only one independent parameter, k_f or k_r, remained to be varied. In this way, NMR line shapes were calculated to reproduce the observed spectra using SPECTRAL ANALYSIS[26] (see Figure 4). The resulting Eyring plot is displayed in Figure 5.

4-Acetyl-1,4-thiazine 1,1-Dioxide (7). 4-Dimethylaminopyridine (200 mg, 1.6 mmol) was added to a mixture of 4*H*-1,4-thiazine 1,1-dioxide[16,27] (5 g, 38 mmol), 10 mL of acetic anhydride, and 20 mL of pyridine at 40 °C. The mixture was heated at 50 °C for 15 min at which time it was poured over ice. A quantity of 4.55 g of white crystals was collected by vacuum filtration in 69% crude yield. Recrystallization in benzene or ethyl acetate yielded pure **7**, mp 160–162 °C: ^1H NMR ($(CD_3)_2CO$, 90 MHz) δ 2.55 (3 H, CH_3), 6.25 (dm, J = 9 Hz, 2 H, SCH), 7.85 (dm, J = 7 Hz, NCH); IR (KBr) 410 (s), 510 (s), 667 (s), 940 (S), 1100 (s), 1260 (bs), 1378 (s), 1636 (C=C), 1724 (s, C=O), 3060 (m), 3100 (m).

4-Acetyl-2,3-dihydro-1,4-thiazine 1,1-Dioxide (8a and 8b). To 4-acetyl-1,4-thiazine 1,1-dioxide (**7**) (2.83 g, 0.0163 mmol) in 210 mL of ethyl acetate was added 280 mg of 5% Pd on carbon. The mixture was hydrogenated at 45 psi in a Parr shaker until 1.75 equiv of H_2 (calculated using the ideal gas law) had been taken up. Note: the catalyst had not been preconditioned with H_2. Celite was added to disperse the catalyst. After filtration of the catalyst and removal of 100 mL of solvent, yellow crystals formed which were recrystallized several times from ethyl acetate to yield 0.56 g of pure 4-acetyl-2,3-dihydro-1,4-thiazine 1,1,-dioxide (**8**) as clear crystals, mp 134–136 °C. After removal of the rest of the solvent a yellow amorphous solid remained, which is a mixture of half-hydrogenated material (**8a,b**), starting material (**7**), and fully hydrogenated material, 4-acetyl-2,3,5,6-tetrahydro-1,4-thiazine 1,1-dioxide (**9**). Column chromatography (active silica gel, ethyl acetate/acetone) was used to separate the mixture with **9** eluting first, followed by **8** and finally **7**. The overall yield of **8a,b**, was 25% (not optimized): ^1H NMR ($(CD_3)_2CO$, 500 MHz, 303 K) δ 2.35 (s, 3 H, CH_3), 3.28 (m, 2 H, SCH_2), 4.33 (m, 2 H, NCH_2), 5.67 (m, 1 H, SCH), 7.55 (m, 1 H, NCH); ^{13}C NMR ($(CD_3)_2CO$, 75.5 MHz, 297 K) δ 21.4 (CH_3), 40, 44.5, 48.8 (CH_2), 106.7, 108, 133, 135.8 (CH), 169.6 (CO); IR (KBr) 3070 (s), 1688 (s, C=O), 1600 (s, C=C), 1380 (s), 1330–1270 (bs), 1105 (s), 860 (m) cm^{-1}; EI MS *m/e* (obsd) 175.0339, *m/e* (calcd) 175.0304.

4-Acetyl-2,3,5,6-tetrahydro-1,4-thiazine 1,1-Dioxide (9). 4-Acetyl-1,4-thiazine 1,1-dioxide (**7**) (0.5 g, 2.89 mmol), free of 4*H*-1,4-thiazine 1,1-dioxide which poisons the catalyst, in 200 mL of ethyl acetate with 200 mg of 5% Pd on carbon was hydrogenated at 45 psi in a Parr apparatus until hydrogen absorption ceased. Celite was added to disperse the catalyst. After filtration of the catalyst, removal of the solvent, and recrystallization of the residue from 2-propanol, there was obtained 0.22 g of 4-acetyl-2,3,5,6-tetrahydro-1,4-thiazine 1,1-dioxide (**9**), a yellow solid in 43% yield, not optimized, mp 121–124 °C: ^1H NMR ($CDCl_3$) δ 2.12 (s, 3 H, CH_3), 2.99 (m, 4 H, SCH_2), 3.98 (m, 4 H, NCH_2); ^{13}C NMR ($CDCl_3$) δ 21.0 (CH_3); 39.9, 44.5, 51.8, 51.9 (CH_2), 168.9 (CO); IR (KBr) 3460 (m), 1637 (s, C=O), 1440 (s), 1290 (s), 1120 (s), 875 (m) cm^{-1}.

1-Methoxy-1-oxo-3-phospholene (10).[12,13] In a modification of the published procedure,[13] ethylene oxide (70 g, 1.59 mol) at 0 °C was added dropwise from a jacketed addition funnel to a stirred solution of freshly distilled phosphorus trichloride (206 g, 1.5 mol) and copper stearate (0.5 g, 0.79 mmol) cooled to 0 °C with a dry ice/2-propanol bath. Caution:

this step must not be carried out below 0 °C since this retards initiation. The solution was cooled to −30 °C after equilibrium was attained. Dry butadiene at −78 °C (132 mL, 82 g, 1.52 mol) was cannulated into the flask. The resulting mixture was poured under a blanket of argon into a vacuum oven dried, precooled (−30 °C), 450-mL stainless steel Parr bomb equipped with a magnetic stirring bar and a glass liner. Note, a glass bomb is preferred since the steel corrodes slightly under the conditions of this reaction. The bomb was sealed, heated to 100 °C for 12 h with stirring, warmed to 110 °C for 1 h, and then allowed to cool to room temperature. After the bomb was slowly opened, the resulting solution was combined with 200 mL of methylene chloride in an apparatus equipped for magnetic stirring, with a water-cooled condenser, dropping funnel, and $CaCl_2$ drying tube. Methanol (121.5 mL) was added dropwise at −10 °C with stirring. After removal of the solvent in vacuo, the residue was distilled twice, leaving 11 g in 4% yield (not optimized) of 1-methoxy-1-oxo-3-phospholene (**10**), bp 72–74 °C (0.07 Torr) (lit.[13] 64–66 °C (0.2 Torr)). Caution: the residue from the first distillation was a pyrophoric gel. GLC analysis indicated 85% purity. ^{1}H NMR: ($CDCl_3$, 90 MHz, J in Hz) δ 2.26 (d, 4 H, J = 12, CH_2), 3.6 (d, 3 H, $J_{P,H}$ = 12, OCH_3), 5.76 (d, $J_{P,H}$ = 33, 2 H, HCCH) [1.35 (s, impurity)].

3,5-Dihydro-2,6-diethoxy-4-methoxy-1,4-oxaphosphorine 4-Oxide (11). A stirred solution of 1-methoxy-1-oxo-3-phospholene (**10**), from the previous reaction (12.7 g, 0.082 mol) in a mixture of 16.1 mL of ethanol and 80 mL of CH_2Cl_2, was ozonized in a Welshbach ozonator at −78 °C (110 V, 8 psi) until the solution turned blue, 2.2 h. After the addition of 11.3 mL of sulfur dioxide (condensed from a tank) portionwise over 15 s, the ice bath was removed and the mixture was allowed to warm to room temperature overnight, 16 h. The resulting yellow solution was poured into a solution of 38.7 g of Na_2CO_3 in 322 mL of water with 64 g of ice, then stirred for 5 min. After separation of the organic layer, the aqueous layer was extracted twice with 50 mL of methylene chloride. The combined organic layers were first washed with 90 mL of water, then 90 mL of brine, and finally dried over $MgSO_4$. Removal of the solvent left a yellow oil with some white solid, presumably 3,5-dihydro-2,6-diethoxy-4-methoxy-1,4-oxaphosphorine 4-oxide (**11**), which was used in the next step without further purification. Three isomers are formed. Three major peaks were seen in the GLC analysis: ^{1}H NMR ($CDCl_3$, J in Hz) δ 1.3–1.1 (m), 3.8–3.4 (m), 4.6 (d, J = 6), 4.9–4.8 (m), 5.0 (ddd, $J_{P,H}$ = 15, $J_{H,H}$ = 3.6, $J_{H,H}$ = 1), 5.17 (dt, $J_{P,H}$ = 25.5, $J_{H,H}$ = 1.5).

4-Methoxy-1,4-dihydro-1,4-azaphosphorine 4-Oxide (12). Bis(acetal) (**11**), 3,5-dihydro-2,6-diethoxy-4-methoxy-1,4-oxaphosphorine 4-oxide (82 mmol), crude product of previous reaction, with ammonium chloride (4.3 g, 80 mmol) in 350 mL of acetic acid was heated to reflux for 30 min. If the scale of this reaction is increased, impurities form and the yield is decreased. After evaporation of the acetic acid, a brown gummy oil remained which was triturated twice with a solution of 75 mL of diethyl ether and 10 mL of 2-propanol. The resulting gummy solid was dissolved in hot 2-propanol, insoluble particles (NH_4Cl) were removed, and, finally, evaporation of the solvent resulted in an orange solid. This solid was dissolved in hot acetone, insoluble particles were filtered out, and final evaporation of the solvent resulted in 3 g of orange crystals, 4-methoxy-1,4-dihydro-1,4-azaphosphorine 4-oxide (**12**), in 25% yield based on 3-phospholene (**10**), mp 203–205 °C; ^{31}P NMR ($CDCl_3$) δ 20.46; ^{1}H NMR: ($CDCl_3$) δ 2.18 (s, 1 H, NH), 3.32 (d, $J_{P,H}$ = 12.5, 3 H, OCH_3), 5.12 (dm, $J_{H,H}$ = 10.6, 2 H, PCH), 7.25 (ddm, $J_{P,H}$ = 28.8, $J_{H,H}$ = 10.6, 2 H, NCH); ^{13}C NMR (CH_3OD, 75.5 MHz) δ 52.16 (d, $J_{C,P}$ = 5.3, OCH_3), 91.84 (d, $J_{C,P}$ = 131, PC), 141.9 (CO); IR (KBr) 3228, 3137 (s, N–H), 3040–2800 (bs), 1610 (s, C=C), 1496 (m, C=C), 1296 (m, P=O), 1226 (sh, P–O–CH_3), 1150 (s), 1040 (s, P–O–CH_3) cm^{-1}; m/z (obsd) 145.0324, m/e (calcd) 145.0292.

The potassium salt was prepared from the amine using KH in DMSO-d_6.

1-Acetyl-4-methoxy-1,4-azaphosphorine 4-Oxide (13). 4-Methoxy-1,4-dihydro-1,4-azaphosphorine 4-oxide (**12**) (1 g, 6.9 mmol), free of NH_4Cl, was heated to reflux in 10 mL of acetic anhydride for 3 h. The reaction was followed by TLC. Note: in the workup, water should be avoided. The acetic acid and acetic anhydride was removed first by rotary evaporation and then with a vacuum pump (0.02 Torr) leaving a brown oil. The oil was heated to 100 °C with a few drops of water for a few minutes. Further evacuation followed by recrystallization of the resulting oil from ethyl acetate gave 0.85 g of 1-acetyl-4-methoxy-1,4-azaphosphorine 4-oxide (**13**), in 60% yield mp 80–82 °C: ^{1}H NMR ($(CH_3)_2CO$) δ 2.56 (s, 3 H, $COCH_3$), 3.48 (d, $J_{P,H}$ = 15, 3 H, $POCH_3$), 5.55 (dm, $J_{H,H}$ = 11.3, 2 H, PCH), 8.05 (ddm, $J_{P,H}$ = 29.96, $J_{H,H}$ = 11.3, 2 H, NCH); ^{13}C NMR ($(CD_3)_2CO$, 75.5 MHz) δ 22.1 (CCH_3), 51.89 ($J_{C,P}$ = 6.0, OCH_3), 100.9 ($J_{C,P}$ = 129.6, PCH), 138.2 (NCH), 169.8 (CO) (all J in Hz); IR (KBr) 1720.3 (s, C=O), 1628.3 (s, C=C), 1382.1 (m), 1271.4 (s), 1183.2 (s), 1023.8 (s), 796.5 (s) cm^{-1}; m/e (obsd) 187.0405, m/e (calcd) 187.0399.

Acknowledgment. We gratefully acknowledge support of this research by the National Science Foundation, Grant No. CHE 8304636, and in part by the Goodyear Tire and Rubber Co. NMR equipment used in this research was financed in part by the National Science Foundation, the National Institutes of Health, and the Office of Research and Graduate Studies, the Ohio State University. We thank the IBM Development Center, Los Angeles, for a travel grant and use of computer facilities, the National Science Foundation for supporting some calculations at the Pittsburgh Supercomputer Center, as well as the Ohio Supercomputer Center. Finally, we thank Dr. Charles Cottrell, Central Campus Instrumentation Center, The Ohio State University, for invaluable technical advice, and Professor Isaiah Shavitt for an illuminating discussion.

Supplementary Material Available: Tables of structural parameters and Mulliken atomic populations from ab initio calculations compared to experimental values (27 pages). Ordering information is given on any current masthead page.